NJC

PAPER

Check for updates

Label-free colorimetric detection of glutathione by autocatalytic oxidation of o-phenylenediamine based on Au^{3+} regulation and its application

Shaoguang Li, [iD] †*[abc] Huilin Liu,†[abc] Xiaoying Zhang,[abc] Jiasong Cai,[abc] Kunlong Huang,[abc] Bing Chen,[abc] Liying Huang,[abc] Zhen Lin, [iD] [a] Xinhua Lin*[abc] and Hong Yao*[abcd]

A label-free, rapid, and highly sensitive colorimetric assay for the detection of glutathione (GSH) was developed. o-Phenylenediamine (OPD) can be selectively oxidized by Au^{3+} in phosphate buffer to produce light yellow 2,3-diaminophenazine. After the addition of GSH, the autocatalytic redox reaction between OPD and Au^{3+} can be effectively inhibited, resulting in a significant decrease in chroma and absorbance intensity. Reduced absorbance intensity can be used for the quantification of GSH. In addition, this method can achieve the discriminative detection of biothiols, such as cysteine and homocysteine. Based on these findings, a simple colorimetric assay was developed for the detection of GSH in the range of 1 nM to 1 mM with a low detection limit of 0.08 nM. More importantly, this procedure is simple, and the whole assay can be accomplished quickly within 15 min. Additionally, the proposed method was successfully used for the determination of GSH in biological fluids, such as serum samples.

1. Introduction

Glutathione (GSH) is the most abundant intracellular biothiol, and as an important endogenous antioxidant, it plays an important role in cell defense against toxins and free radicals.[1] GSH can be widely involved in immune regulation, human metabolism, energy transport, and other physiological processes. As a result, GSH has been widely used to protect the liver and kidneys for detoxification and anticancer drugs. The abnormal level of GSH has been reported to be closely related to aging and various human diseases, such as cancer, liver damage, human immunodeficiency virus, and diabetes. Accordingly, sensitive detection of GSH with high simplicity is of sustained interest to satisfy clinical and medical requirements.[2]

[a] *Department of Pharmaceutical Analysis, School of Pharmacy, Fujian Medical University, Xue Yuan Road, University Town, Fuzhou, Fujian, 350122, People's Republic of China. E-mail: lsg941@126.com, xhlin1963@sina.com, yauhung@126.com, hongyao@mail.fjmu.edu.cn; Fax: +86 0591 22862016; Tel: +86 13705919466, +86 13906909638, +86 18259171978*
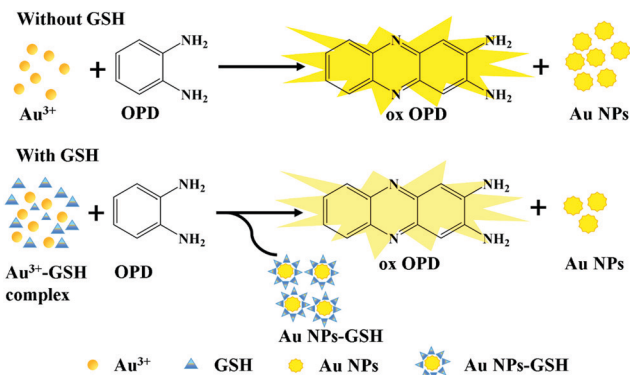
[b] *Higher Educational Key Laboratory for Nano Biomedical Technology of Fujian Province, Fujian Medical University, Fuzhou, 350122, People's Republic of China*

[c] *Nano Medical Technology Research Institute, Fujian Medical University, Fuzhou, 350122, People's Republic of China*

[d] *Fujian Key Laboratory of Drug Target Discovery and Structural and Functional Research, Fujian Medical University, Fuzhou, 350122, People's Republic of China*

† Both authors are equal to this contribution.

To date, various methods have been proposed for the detection of GSH; these methods include fluorescence assay,[3] electrochemical method,[4] high-performance liquid chromatography,[5] surface-enhanced Raman scattering,[6] time-gated luminescence determination,[7] enzyme-linked immunosorbent assay,[8] colorimetric[9,10] and lateral flow assays,[11] high-performance capillary electrophoresis,[12] and magnetic resonance energy transfer.[13] Fluorescence and time-gated luminescence measurement have high requirements for the instrument, whereas electrochemical methods include interference factors. Enzyme-linked immunosorbent assay has high requirements on the state of enzymes and slightly deviates from high-cost enzymes, which will affect the detection results. In addition, most methods fail to reduce the effects of biothiols, such as cysteine (Cys) and homocysteine (Hcy). A simple, low-cost, rapid, and effective GSH detection method that can reduce the interference of Cys, Hcy, and other biological thiols is still one of the directions to be studied urgently.

Colorimetry determines the target analyte content by measuring or comparing solutions of colored substances.[14] Colorimetric assays, possessing unique merits, such as low cost, high sensitivity, and easy operation, have been widely developed for clinical medical diagnosis.[15] Therefore, more people turn to the development of colorimetric methods for GSH detection. However, given its similar functional groups, the selective detection of GSH to reduce the effects of other biological thiols (such as Cys and Hcy) is still challenging for most GSH detection methods. Thus, simpler, more

Scheme 1 Schematic of the color reaction mechanism of OPD.

rapid, and sensitive methods for GSH detection should be developed.

O-Phenylenediamine (OPD) can be readily oxidized by several types of oxidants to generate 2,3-diaminophenazine (oxidized OPD, ox OPD),[16] which exhibits fluorescence and absorption signals.[17] As an important colorimetric and fluorescent sensor, OPD has been utilized to develop a series of assays for relevant reactants.[18,19] In this work, we have developed a color reaction based on the OPD for the detection of GSH. The color reaction is triggered by Au^{3+}, and OPD can be oxidized to ox OPD. As shown in Scheme 1, OPD can be selectively oxidized by Au^{3+} in phosphate buffer to produce a light-yellow ox OPD. When GSH was added, the autocatalytic redox reaction between OPD and Au^{3+} can be effectively inhibited, resulting in significant decrease in chroma and absorbance intensity. This result is mainly due to the possible chelation of Au^{3+} by GSH to inhibit the oxidation capability of Au^{3+} to OPD oxidation reaction.[20] The decrease in absorbance intensity can be used to quantify GSH.[21] Therefore, a label-free colorimetric assay for the highly sensitive and selective determination of GSH has been developed innovatively. More importantly, the method showed that the selective response to GSH was higher than that to Cys, Hcy, and other amino acids. Finally, the method was applied to the determination of GSH in real samples.

2. Experimental section

2.1. Materials and instruments

GSH (reduced form) was obtained from Beijing Bailingwei Technology Co. Ltd (Beijing, China). OPD, $Na_2HPO_4 \cdot 12H_2O$, $NaH_2PO_4 \cdot 2H_2O$, NaCl, HCl, NaOH, and L-Cys were purchased from Sinopharm Chemical Reagent Co. Ltd (Shanghai, China). $HAuCl_4 \cdot 3H_2O$ and L-Hcy were purchased from Aladdin Reagent Co. Ltd (Shanghai, China). Isoproterenol was purchased from Sigma-Aldrich Reagent Co. Ltd (St. Louis, MO, USA). All the solutions were prepared using the ultrapure water generated by a Millipore Milli-Q water purification system (Billerica, MA, USA) with an electric resistance ≥ 18.2 MΩ.

Transmission electron microscopy (TEM) images were acquired on a JEM-2100 electron microscope (JEOL, Japan). Ultraviolet-visible light (UV-vis) absorption spectra were

recorded at room temperature on a UV-2600 spectrophotometer (Shimadzu, Japan). The pH was recorded with a PHSJ-4F acidometer (Thunder Magnetic, Shanghai).

2.2. Detection of GSH

A total of 25 μL 0.75 mM $HAuCl_4 \cdot 3H_2O$ was dispersed in 0.6 mL pH 5.0 phosphate buffer solution (0.01 M) and then added with 200 μL GSH of different concentrations. Finally, 50 μL 2 mM OPD was added. After incubation at 10 °C for 15 min (under light-proof conditions) with a thermostat, the reaction system was transferred for UV-vis detection. The linear range was 1 nM to 1 mM ($r = 0.9994$).

2.3. Selectivity investigation

A selectivity study was performed as follows: various interferents, including L-Cys, L-Hcy, L-Val, L-Lys, L-Ser, L-Ala, DL-Cit, DL-Tyr, L-Pro, DL-Trp, L-Gly, L-Arg, L-Leu, L-His, DL-Met, L-Phe, L-Ile, L-Gln, UA, and AA, and metal cations, such as K^+, Na^+, Ag^+, Ca^{2+}, Zn^{2+}, Cu^{2+}, Mg^{2+}, Cr^{3+}, Co^{2+}, Cd^{2+}, Mn^{2+}, Pb^{2+}, Ni^+, Fe^{2+}, and Fe^{3+}, were explored in the reaction system.

2.4. Detection of GSH in actual samples

Adult male SD rats (weighing 180–200 g) were purchased from Fujian Medical University Laboratory Animal Center and housed in a clean grade room at 23 ± 2 °C and $50\% \pm 5\%$ humidity under a 12 h light–dark cycle with free access to food and water. All animal procedures were performed in accordance with the Guidelines for Care and Use of Laboratory Animals of Fujian Medical University and experiments were approved by the Animal Ethics Committee of Fujian Medical University.

The animals were randomly divided into two groups (3 mice in each group): the model and control groups. An acute myocardial injury model of SD rats was established by subcutaneous injection (back of the neck) of 0.5 mL 0.004 g mL^{-1} isoproterenol, whereas the control group was injected with the same volume of normal saline. At 0 and 10 min and 0.5, 1, 2, 4, 8, 12, and 24 h after injection, 300 μL blood was obtained from the tail vein of the rat. Serum was obtained by centrifugation at 2500 rpm min^{-1} for 10 min at 4 °C, followed by dilution for 100 times and immediate detection of GSH.

3. Results and discussions

3.1. Feasibility analysis of GSH determination

The different absorbances were displayed in the system with and without GSH. The addition of GSH decreased the absorbance of the system and lightened its color (Fig. 1a), which can be used for colorimetric determination. When Au^{3+} was replaced with other metal cations, no similar phenomenon was recorded in the OPD system (Fig. 1b). According to previous reports, several metal ions, such as Ce^{4+}, Cu^{2+}, Ag^+, and Fe^{3+}, have the oxidation capability to oxidate OPD,[22–25] and the generated metal nanoparticles (NPs) can catalyze the reaction between OPD and metal ions;[26] in our work, these interference metal ions barely responded to our sensing system, possibly due to the different
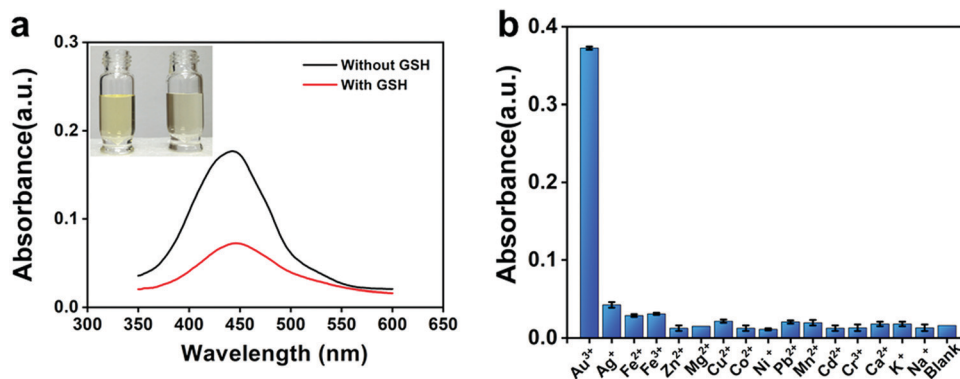
Fig. 1 (a) UV-vis absorption spectrum of Au^{3+}–OPD solution in the absence of GSH and 10 μM GSH. Insets exhibit the corresponding photographs under visible light. (b) Selectivity of OPD reaction system to different metal ions. The concentrations of OPD and metal ions were 2 mM and 1 mM, respectively.

conditions of the sensing system, such as the absence of hydrogen peroxide, blue-light proof, low concentrations of reactants, and a short incubation time. In addition, the capability of OPD to cause the aggregation of Au NPs through NH–Au bond[27] may explain how Au NPs catalyze the oxidation reaction. Therefore, we speculate that based on the Au^{3+}–OPD reaction system, a new, label-free, colorimetric method can be proposed for the determination of GSH.

3.2. Characterization of Au NPs and ox OPD

The effect of GSH on the reaction between Au^{3+} and OPD was further studied by TEM. The TEM results showed that the Au NPs produced in the presence of GSH (Fig. 2b and c) were completely different in size and shape from those produced in the absence of GSH (Fig. 2a). The results showed that GSH had an effect on the redox reaction between OPD and Au^{3+} and further affected the synthesis of Au NPs. In addition, GSH may

coat the surface of Au NPs through strong Au–S bonds,[28] resulting in changes in the surface properties of Au NPs; these Au–S bonds may replace the NH–Au bonds during the reaction process and cause Au NPs to have a weak catalytic effect on the Au^{3+}–OPD reactions.[29]

As shown in Fig. 2d, the ox OPD exhibited a strong fluorescence, with an excitation wavelength of 420 nm and an emission wavelength of 568 nm. As shown in Fig. 2e, the OPD showed no absorption at 447 nm and presented an absorption peak at 288 nm, whereas the ox OPD had a significant absorption peak at 447 nm.

3.3. Optimization of experimental conditions

To achieve the optimum performance for GSH detection, we optimized important detection conditions, including pH, reaction time, temperature, and the concentrations of OPD and $HAuCl_4$. The change in absorbance ΔA ($\Delta A = A_0 - A$) was used as a parameter to optimize detection conditions, where A_0
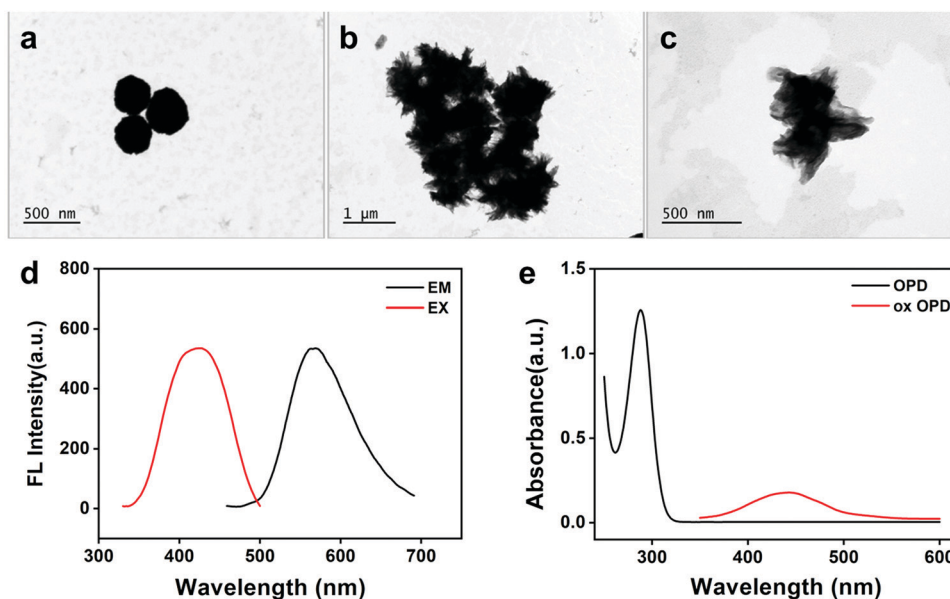

Fig. 2 (a) TEM graph without GSH. (b and c) TEM graphs with GSH. (d) Fluorescence spectrum of ox OPD. (e) UV-vis absorption spectrum of OPD and ox OPD.

and A represent the intensity of absorbance at 447 nm in the absence and presence of GSH, respectively. The effect of pH on the ΔA value was first studied by using phosphate buffers with different pH (Fig. 3a). The reaction system was incubated with a thermostat at 35 °C. Then, the absorbance of the reaction system was measured by UV-vis spectrophotometer every 5 min. The results obtained after 15 min were plotted as a line chart (Fig. 3b). A strong basicity or strong acidity largely influences the reaction system, but in the reaction system of pH 5.0 starting from 15 min, the system was stable and exhibited a prolonged plateau period (Fig. 3a, green trend line). Therefore, a phosphate buffer system of pH 5.0 was finally selected, and the reaction time was 15 min. Fig. 3c shows the effect of different incubation temperatures on ΔA from 0 °C to 50 °C. The ΔA reached a peak value at 10 °C. Therefore, 10 °C was selected as the reaction temperature of the system.

Next, the ΔA value was investigated at OPD concentrations ranging from 0.5 mM to 4 mM, and the results are shown in Fig. 3d. When the OPD concentration was 2 mM, the maximum ΔA was obtained. Therefore, 2 mM OPD was selected as the optimal concentration in the following experiments. In the experiments, Au^{3+} concentration played an important role in the selective detection of GSH on Cys and Hcy. The effect of Cys was greater than that of Hcy. Therefore, Cys was used to simulate the environment of biothiol. By setting different concentrations of $HAuCl_4\cdot3H_2O$, we investigated the effect of Au^{3+} concentration on $\Delta A GSH/|\Delta A Cys|$ in the presence of Cys (Fig. 3e). The high ratio of $\Delta A GSH/|\Delta A Cys|$ indicates that the proposed detection method can detect GSH with high selectivity on Cys. When the Au^{3+} concentration was 0.75 mM, $\Delta A GSH/|\Delta A Cys|$ attained a maximum value. Therefore, 0.75 mM Au^{3+} was selected for detection of GSH.

3.4. Analytical performance of colorimetric assay

Under the above optimized determination conditions, we investigated the sensitivity of the proposed method by exposing it to a series of different GSH concentrations (0, 1.14, 5.71, 11.43, 57.14, 114.29, 571.43, 1142.86, 5714.29, 11428.57, 57142.86, and 114285.71 nM). Fig. 4a depicts the typical absorbance spectra of the colorimetric biosensor to GSH at varying concentrations. The absorbance signals gradually decreased as the concentration of GSH varied from 0 mM to 1 mM. Therefore, as the GSH concentration increased, the ΔA value increased systematically and reached the highest value when the GSH concentration reached 1 mM (Fig. 4b). The logarithm of the ΔA value was linear to that of the GSH concentration, ranging from 1 nM to 1 mM (regression coefficient R^2 = 0.9988) (Fig. 4b, inset). The linear regression equation is $y = -2.0175 + 0.2950x$, where x is the logarithm of the GSH concentration, and y is the logarithm of the ΔA value. The relative standard deviation of 10 μM GSH in five repeated tests was 2.2%, indicating that the proposed GSH assay has good reproducibility and reliability. The limit of detection (LOD) was as low as 0.08 nM, and the signal-to-noise ratio was 3 (S/N = 3); such a good sensitivity may be due to the strong molar extinction coefficient of ox OPD ($\varepsilon = 2.1 \times 10^4$ $M^{-1}\cdot cm^{-1}$,[30]). Previous literature[26,31,32] confirmed that the target reactant can be detected in nanomolar concentrations through an OPD-based sensor. Compared with several reported methods based on other nanomaterials,[33–36] our method has lower LOD and higher sensitivity. The details of the proposed method, including LOD, linear range, and analysis time were compared with those of different sensing platforms, and the results are shown in Table 1. The low LOD and relative standard deviation demonstrated that the developed colorimetric assay can be used successfully for sensitive GSH detection with a simple experimental procedure.
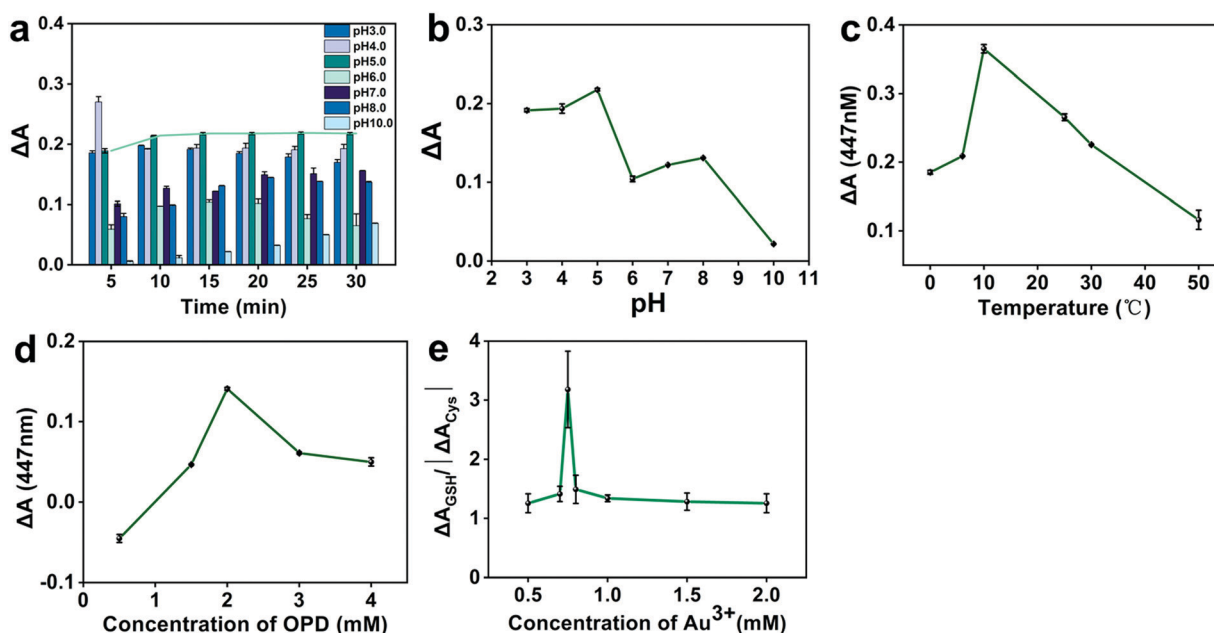

Fig. 3 (a) Effect of different pH with time on ΔA. (b) Effect of pH on ΔA. (c) Effect of different temperatures on ΔA. (d) Effect of different OPD concentrations on ΔA. (e) Effect of different Au^{3+} on $\Delta A GSH/|\Delta A Cys|$.
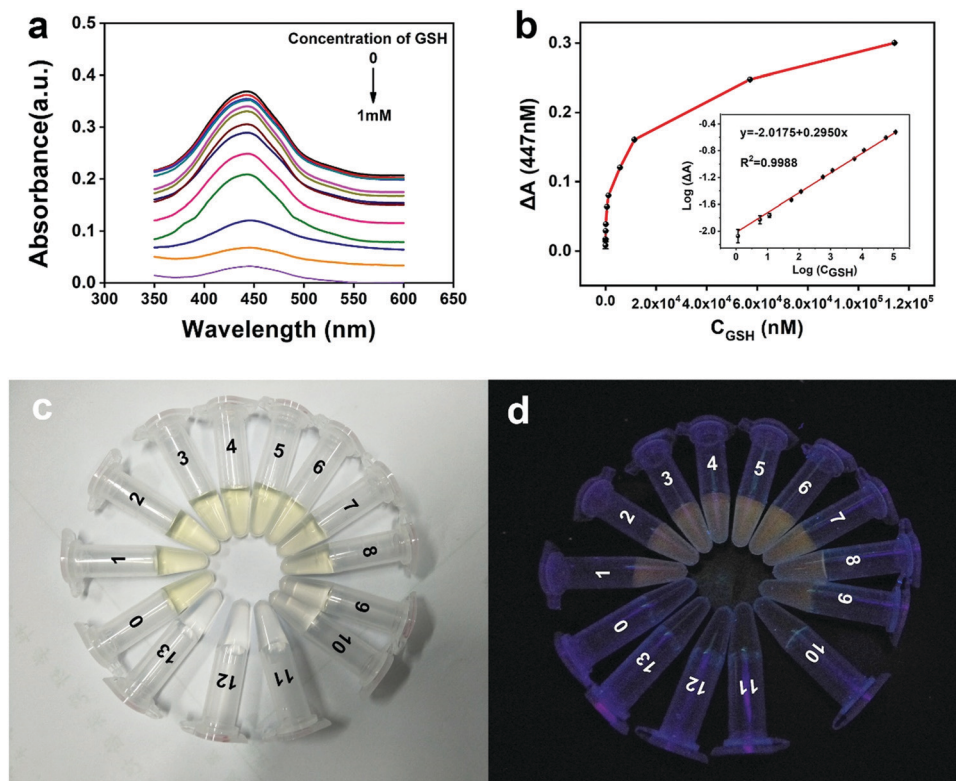
Fig. 4 (a) Absorption spectra of Au^{3+}–OPD solution with the increase in concentration of GSH in the range of 0–1 mM. (b) Relationship between ΔA and GSH concentration. Inset: Linear calibration of GSH detection. (c) Visible-light pattern of Au^{3+}–OPD solution in the presence of different concentrations of GSH (0–13 : 0, 1.14, 5.71, 11.43, 57.14, 114.29, 571.43, 1142.86, 5714.29, 11428.57, 57142.86, and 114285.71 nM). (d) UV image at 365 nm.

3.5. Evaluation of detection selectivity

The selectivity of the proposed GSH determination method was further investigated. First, we established two blank controls based on the previously optimized conditions, namely, without interference and with GSH as a negative control and without interference but with GSH as a positive control. Then, based on these blank controls, different kinds of interferents were added to investigate the selectivity of the proposed method (the concentration and volume of interferents and GSH were 1 mM and 200 μL, respectively). The absorbance was measured to evaluate the effect of interferents, and the results are shown in Fig. 5. In the presence of interfering substances, especially in the presence of the detection substance GSH, a minimal effect was observed on the absorbance of the reaction system. In addition, in this work, Cys and Hcy showed minimum influence, whereas in previous reports, the detection signals in the presence of Cys and Hcy were similar to or higher than that of GSH.[34–37] Meanwhile, the proposed colorimetric assay

showed a high selectivity for GSH detection of potential interferents, including competitive biothiols such as Cys and Hcy. To the best of our knowledge, this selectivity may be attributed to several possible reasons. Given that the mechanism of OPD-based sensor is redox reaction, GSH has a better reduction activity than Cys and Hcy;[33] thus, GSH is more likely to respond to the sensing system. Compared with Cys and Hcy, GSH contains more electron-rich group,[38] has a longer distance between the sulfhydryl group and amido group,[39] and has a larger steric hindrance effect;[40] thus, when biological thiols coat the surface of Au NPs and weaken the catalytic effect of Au NPs, GSH can exhibit a better inhibition capability on the autocatalytic reaction.

3.6. Determination of actual samples

The good sensitivity, simplicity, and selectivity of our method suggest that it may be directly applied for GSH determination in real samples. This colorimetric method was used to detect

Table 1 Comparison of different sensing platforms

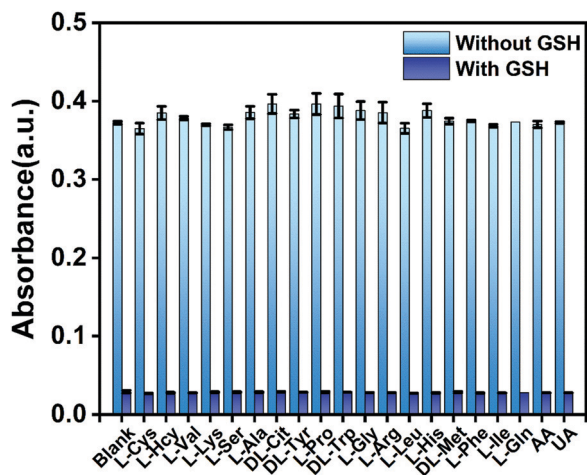| Sensing system	Method	Linear range (mM)	LOD (mM)	Time (min)	Ref.
Ag^+-TMB	Colorimetric	0.05–8	0.05	10	33
CQDs-Au NPs	Colorimetric	1.0–4.0	—	5	34
PEI-capped Ag NCs	Fluorimetry	0.5–6.0	0.38	30	35
Au NCs-Hg (II)	Fluorimetry	0–250	9.4×10^{-6}	21	36
Au^{3+}-OPD	Colorimetric	1×10^{-6}–1	0.08×10^{-6}	15	Our work

Fig. 5 Selectivity of GSH upon the introduction of different interferents.

GSH in serum samples from a rat myocardial ischemia–reperfusion model. The serum samples were diluted 100 times with phosphate buffered saline to ensure that the GSH concentration was within the linear range. Then, GSH was determined by the standard curve method. As shown in Fig. 6a, electrocardiograms (ECGs) were measured at regular intervals to monitor the changes in cardiac electrical activity in each cardiac cycle induced by isoproterenol.

As shown in Fig. 6b, the concentration of GSH in the serum of the control group rats did not change significantly, and

slight fluctuations, which were acceptable, were observed. In the model group, a strong GSH concentration peak was observed 1 h after the injection of isoproterenol, and it then dropped rapidly in the next hour, which is a pathological manifestation of acute cardiac reperfusion. In addition, the GSH levels in the mice of model and control groups have risen at the time points of 10 min and 8 h. According to a previous report,[41] within a certain period, the blood GSH level fluctuations in the range of 0.30 mM to 0.99 mM normalize, which also confirms that the acute cardiac reperfusion injury model was successfully established. Therefore, the proposed colorimetric method was successfully applied in real samples. Then, the concentration of GSH was spiked in the plasma samples, and the acceptable recoveries (102.6%) and relative standard deviation (2.43%) confirmed the good accuracy and reliability of the GSH detection method.

4. Conclusions

In summary, we developed a rapid, selective, and sensitive label-free colorimetric method for GSH detection based on Au^{3+}-regulated OPD autocatalytic oxidation reactions. The as-proposed colorimetric method provides a wide linear range from 1 nM to 1 mM, a low LOD of 0.08 nM for GSH assay, and a shortened detection time. The discriminant detection of biological thiols, such as Cys and Hcy, has been realized. The developed method is superior to previously reported
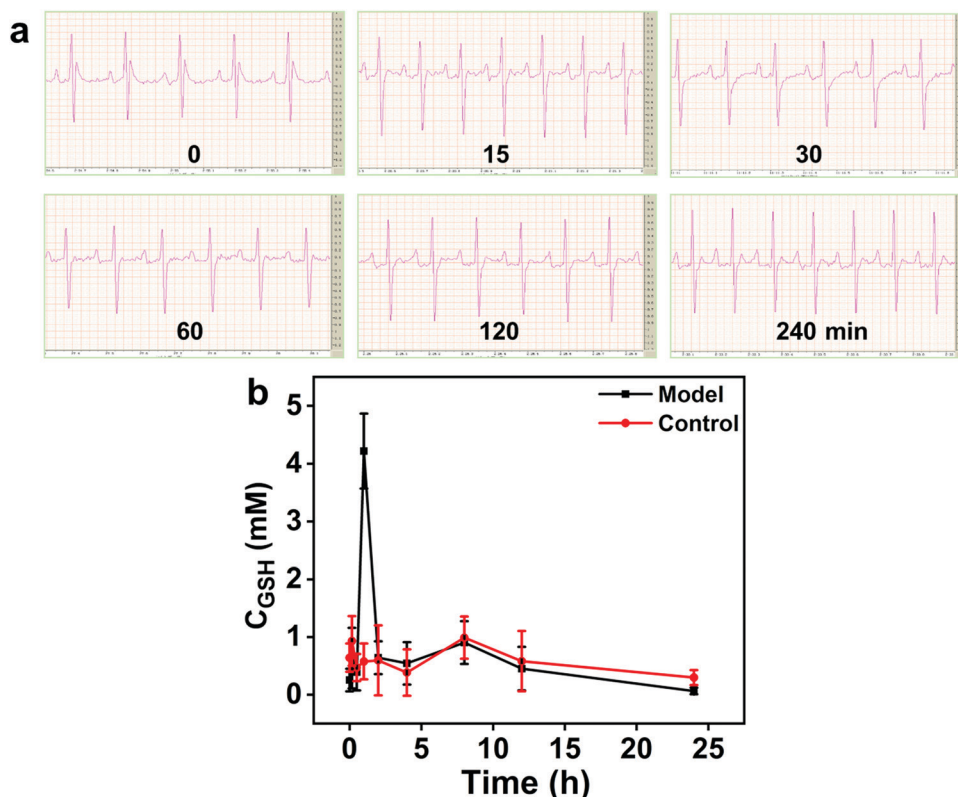

Fig. 6 (a) ECGs of model rat (0–240 min). (b) Changes in serum GSH concentration in the rat model of myocardial ischemia–reperfusion (0–24 h, $n = 6$).

procedures in terms of simplicity, sensitivity, selectivity, and efficiency.

In addition, during the application of this method in the detection of biological samples, GSH in the blood of rats with acute myocardial injury peaked at 1 h after the occurrence of the injury and returned to normal levels at about 2 h. This finding is consistent with the ECG monitoring data and provides a detailed reflection of the body-to-acute injury stress response level, thus providing a useful guiding significance in clinical prevention and treatment.

Conflicts of interest

There are no conflicts to declare.

Acknowledgements

References

1 R. R. Deng, X. J. Xie, M. Vendrell, Y. T. Chang and X. G. Liu, *J. Am. Chem. Soc.*, 2011, **133**, 20168–20171.

2 Q. Y. Cai, J. Li, J. Ge, L. Zhang, Y. L. Hu, Z. H. Li and L. B. Qu, *Biosens. Bioelectron.*, 2015, **72**, 31–36.

3 Z. Q. Zhang, T. T. Liu, S. S. Wang, J. Ma, T. Zhou, F. Wang, X. F. Wang and G. D. Zhang, *J. Photochem. Photobiol., A*, 2019, **370**, 89–93.

4 H. P. Peng, M. L. Jian, Z. N. Huang, W. J. Wang, H. H. Deng, W. H. Wu, A. L. Liu, X. H. Xia and W. Chen, *Biosens. Bioelectron.*, 2018, **105**, 71–76.

5 D. L. Rabenstein and R. Saetre, *Anal. Chem.*, 1977, **49**, 1036–1039.

6 W. K. Wang, L. M. Zhang, L. Li and Y. Tian, *Anal. Chem.*, 2016, **88**, 9518–9523.

7 Q. K. Gao, W. Z. Zhang, B. Song, R. Zhang, W. H. Guo and J. L. Yuan, *Anal. Chem.*, 2017, **89**, 4517–4524.

8 N. K. Wawegama, G. F. Browning, A. Kanci and M. S. Marenda, *Clin. Vaccine Immunol.*, 2014, **21**, 196–202.

9 J. Ge, R. Cai, X. G. Chen, Q. Wu, L. L. Zhang, Y. Jiang, C. Cui, S. Wan and W. H. Tan, *Talanta*, 2019, **195**, 40–45.

10 Z. M. Huang, Q. Y. Cai, D. C. Ding, J. Ge, Y. L. Hu, J. Yang, L. Zhang and Z. H. Li, *Sens. Actuators, B*, 2017, **242**, 355–361.

11 J. Chen, Z. M. Huang, H. M. Meng, L. Zhang, D. Y. Ji, J. Z. Liu, F. Yu, L. B. Qu and Z. H. Li, *Sens. Actuators, B*, 2018, **260**, 770–777.

12 F. Carlucci, A. Tabucchi, B. biagioli, G. Sani, G. Lisi, M. Maccherini, F. Rosi and E. Marinello, *Electrophoresis*, 2020, **21**(8), 1552–1557.

13 K. Wang, H. L. Zhang, A. J. Shen, P. R. Zhao, X. F. Meng, X. Y. Chen, Y. Liu, Y. Y. Liu, T. Gong, W. L. Wu, X. M. Fang, P. J. Wang and W. B. Bu, *Biomaterials*, 2020, 232.

14 Y. L. Xianyu, Y. Z. Y. Xie, N. X. Wang, Z. Wang and X. Y. Jiang, *Small*, 2015, **11**, 5510–5514.

15 Q. Liu and J. Wang, *Talanta*, 2015, **136**, 114–127.

16 R. P. Doyle, P. E. Kruger, P. R. Mackie and M. Nieuwenhuyzen, *Acta Crystallogr., Sect. C: Cryst. Struct. Commun.*, 2001, **57**(Pt 1), 104–105.

17 L. Deng, Q. Q. Liu, C. Y. Lei, Y. Y. Zhang, Y. Huang, Z. Nie and S. Z. Yao, *Anal. Chem.*, 2020, **92**(13), 9421–9428.

18 Q. X. Ye, S. F. Ren, H. Huang, G. G. Duan, K. M. Liu and J. B. Liu, *ACS Omega*, 2020, **5**(33), 20698–20706.

19 J. Sun, B. Wang, X. Zhao, Z. J. Li and X. R. Yang, *Anal. Chem.*, 2016, **88**(2), 1355–1361.

20 Y. R. Tang, H. J. Song, Y. Y. Su and Y. Lv, *Anal. Chem.*, 2013, **85**, 11876–11884.

21 X. Liu, Q. Wang, Y. Zhang, L. C. Zhang and Y. Lv, *New J. Chem.*, 2013, **37**, 2174–2178.

22 M. Xia, X. E. Zhao, J. Sun, Z. J. Zheng and S. Y. Zhu, *Sens. Actuators, B*, 2020, **319**, 128321.

23 X. Yang and E. K. Wang, *Anal. Chem.*, 2011, **83**(12), 5005–5011.

24 W. F. Deng, Y. Peng, H. Yang, Y. M. Tan, M. Ma, Q. J. Xie and S. W. Chen, *ACS Appl. Mater. Interfaces*, 2019, **11**(32), 29072–29077.

25 J. K. Liang, H. Li, J. R. Wang, H. L. Yu and Y. He, *Anal. Chem.*, 2020, **92**(9), 6548–6554.

26 J. H. Yang, Y. Zhang, L. Zhang, H. L. Wang, J. F. Nie, Z. X. Qin, J. Li and W. C. Xiao, *Chem. Commun.*, 2017, **53**(54), 7477–7480.

27 Y. L. Li, Y. M. Leng, Y. J. Zhang, T. H. Li, Z. Y. Shen and A. G. Wu, *Sens. Actuators, B*, 2014, **200**, 140–146.

28 S. Chakrabarty, S. Maity, D. Yazhini and A. Ghosh, *Langmuir*, 2020, **36**(38), 11255–11261.

29 H. C. Dai, P. J. Ni, Y. J. Sun, J. T. Hu, S. Jiang, Y. L. Wang and Z. Li, *Analyst*, 2015, **140**, 3616–3622.

30 N. Tyagi and P. Mathur, *Spectrochim. Acta, Part A*, 2012, **96**, 759–767.

31 Y. Zhou and Z. F. Ma, *Sens. Actuators, B*, 2017, **249**, 53–58.

32 J. H. Wang, H. Li, Y. H. Cai, D. J. Wang, L. Bian, F. Q. Dong, H. L. Yu and Y. He, *Anal. Chem.*, 2019, **91**, 6155–6161.

33 P. J. Ni, Y. J. Sun, H. C. Dai, J. T. Hu, S. Jiang, Y. L. Wang and Z. Li, *Biosens. Bioelectron.*, 2015, **63**, 47–52.

34 Y. P. Shi, Y. Pan, H. Zhang, Z. M. Zhang, M. J. Li, C. Q. Yi and M. S. Yang, *Biosens. Bioelectron.*, 2014, **56**, 39–45.

35 N. Zhang, F. Qu, H. Q. Luo and N. B. Li, *Biosens. Bioelectron.*, 2013, **42**, 214–218.

36 K. S. Park, M. I. Kim, M. A. Woo and H. G. Park, *Biosens. Bioelectron.*, 2013, **45**, 65–69.

37 Q. Zhang, D. H. Yu, S. S. Ding and G. Q. Feng, *Chem. Commun.*, 2014, **50**, 14002–14005.

38 X. D. Zhang, F. G. Wu, P. D. Liu, N. Gu and Z. Chen, *Small*, 2014, **10**(24), 5170–5177.

39 H. Li, Y. Z. Yang, X. Y. Qi, X. G. Zhou, W. X. Ren, M. M. Deng, J. M. Wu, M. H. Lv, S. C. Liang and A. T. Teichmann, *Anal. Chim. Acta*, 2020, **1117**, 18–24.

40 H. S. Jung, X. Q. Chen, J. S. Kim and J. Y. Yoon, *Chem. Soc. Rev.*, 2013, **42**(14), 6019–6031.

41 G. Calcutt, *Naturwissenschaften*, 1967, **54**, 120.